Birefringence-induced interference effects in thin-film magnetic-circular-dichroism spectra

Dennis Rioux and Brian Allen
Department of Physics and Astronomy, University of Wisconsin-Oshkosh, 800 Algoma Boulevard, Oshkosh, Wisconsin 54901-8644

Hartmut Höchst, Dai Zhao, and David L. Huber
Synchrotron Radiation Center, University of Wisconsin-Madison, 3731 Schneider Drive, Stoughton, Wisconsin 53589-3097
(Received 2 December 1996)

Magnetic-circular-dichroism (MCD) spectra taken at the $M_{2,3}$ absorption edge of thin Fe films exhibit pronounced thickness-dependent variations in the MCD signal and line shape which are related to birefringence effects in the ferromagnetic film. Model calculations based on the Maxwell-Fresnel formalism are used to calculate the different interference effects occurring for left- and right-circularly polarized light reflected from the vacuum/film/substrate interfaces. The $M_{2,3}$ MCD experiments confirm the magnitude- and thickness-dependent periodicity predicted by the macroscopic theory. The data clearly demonstrate the importance of the interference effects which are very pronounced for film thicknesses up to several units of the excitation wavelength λ. While at the Fe $M_{2,3}$ transition the thickness corresponding to the wavelength unit is about 220 Å, the same effects are to be expected in the Fe $L_{2,3}$ spectra for considerably thinner films since the wavelength is only λ~17 Å. The observed interference effects are of general character and caution should be employed in attempts to relate changes in the $L_{2,3}$ MCD spectra of several-monolayer thin films solely to the formation or reorientation of magnetic moments and to their decomposition into spin and orbital components. Because the theory employed here considers the total power dissipated in the reflection and absorption processes rather than amplitudes of reflected waves, interference effects are not restricted to reflection MCD measurements, but should also be present in a slightly modified form in the more commonly used total-electron-yield-type absorption MCD experiment. [S0163-1829(97)05426-X]

INTRODUCTION

X-ray magnetic circular dichroism is a relatively new magneto-optical experimental technique[1–3] designed to probe the local magnetic structure of ferromagnetically ordered materials using circularly polarized x rays. As scientists seek to tailor magnetic properties at the atomic level by growing thin-film multilayer structures and compound ferromagnetic materials, they are increasingly turning to magnetic circular dichroism (MCD) to characterize these samples.[4] Dichroism spectra from absorption edges, most often the $L_{2,3}$ and $M_{2,3}$ edges, give MCD the chemical specificity that is necessary to evaluate the new complex multicomponent materials. Among the properties probed by this technique are the magnitude and orientation of magnetic moments,[5] their degree of localization or itineracy,[3,6] and differences between surface and bulk magnetizations.[7] A number of advances in theoretical approach[8–10] have increased the utility of the sum rules that relate features of experimental MCD spectra to microscopic magnetic properties of the magnetic moment, although some controversy still exists over their implementation.[11–14]

While MCD theories quickly advanced to incorporate many-electron effects, surprisingly little attention was paid to the optical part of the process, e.g., partial phase shifts at material interfaces and different polarization dependences of the refracted light wave in ferromagnetic films. In addition to the well-known dependence of MCD on the relative orientation between the helicity of the incident light and the magnetization vector **M**, calculations made using a classical, dielectric model of thin-film interference show that film thickness plays an important role in the measured MCD signal. Using the relatively simple Maxwell-Fresnel approach, we show that interference effects which arise from different contributions for left- and right-circularly polarized light reflected from the vacuum-film and the film-substrate interfaces (see Fig. 1) result in thickness-dependent modulation

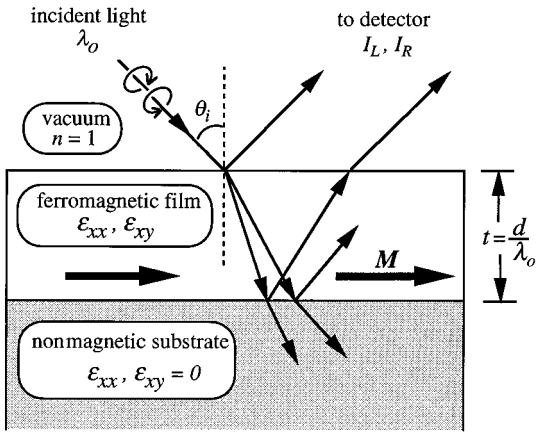

FIG. 1. Schematic of a MCD experiment in the longitudinal geometry in which the magnetization **M** of the sample lies in the plane of the film surface and in the plane of incidence defined by the light ray and the surface normal. Governed by the off-diagonal elements ϵ_{xy} of the dielectric tensor, LCP and RCP rays are refracted differently within the film, leading to interference patterns that depend on the helicity of the light in addition to the film thickness (reported in dimensionless units normalized to the incident wavelength $t=d/\lambda$).

 © 1997 The American Physical Society

of MCD spectra. These processes contribute to the experimental signal and, if ignored, cause difficulties in extracting meaningful material properties from MCD spectra.

We have used reflection MCD to specifically study these effects. To decouple the issues of varying magnetic properties at interfaces and films of several monolayer thickness from the optical contributions such as differences in the interference effects of left- and right-circularly polarized radiation, we chose to study the $M_{2,3}$ edge of Fe rather than the better understood $L_{2,3}$ transition. The reasoning for this decision is straightforward. Since the thickness dependence of the interference effects scale with the excitation wavelength, the effects at the Fe $M_{2,3}$ transition at $\sim$54 eV occur at approximately 13 times the thickness compared to the same experiment studied at the $L_{2,3}$ transition at $\sim$720 eV. This increase in wavelength allows us to study the effects of interest in considerably thicker films (hundreds of Å) where the magnetic properties have reached bulklike behavior which is in contrast to pursuing the same experiment at the $L_{2,3}$ edge where unknown material and interface properties at the monolayer regime (tens of Å) can influence the results.

It must be noted, however, that the film-thickness- and angle-dependent interference effects are not restricted to spectra collected in the reflected light mode—the theoretical calculations utilize a total-power calculation that implies MCD spectra obtained from absorbed light will also exhibit thickness-dependent interference effects. We present here an outline of the theoretical model and our experimental confirmation of the predicted interference effects in the MCD spectrum of ferromagnetically ordered Fe films.

EXPERIMENT

MCD spectra were collected at the University of Wisconsin's Synchrotron Radiation Center using monochromatic, circularly polarized x rays supplied by a quadruple reflection polarizer[15] (QRP) attached to the exit mirror box of the Amoco 6-m toroidal grating monochromator.[16] The QRP converts the linearly polarized light passed by the beam line optics to circularly polarized light by inducing phase shifts between s- and p-polarized components of the light. Verification of the proper operation of the QRP and its utility in MCD measurements can be found elsewhere.[17,18]

Thin Fe films were grown under ultrahigh-vacuum conditions and at room temperature on Si(100) substrates using an electron-beam evaporator, and film thickness was monitored with a quartz microbalance. To prevent reaction and interdiffusion between the Fe films and Si substrates, a 200-Å layer of Cu was first deposited. The Cu-Fe interface is known to be more abrupt than the Fe-Si interface,[19–21] and we noted a marked increase in signal quality over films grown on bare Si(100) substrates. Even though the Fe films were grown by molecular-beam-epitaxy (MBE) techniques on a single-crystal substrate, it is not assumed that this would lead to an ordered overlayer growth of Fe of several hundred Å thickness. The issue of interest here is to grow a reasonably smooth film on a nonreactive substrate rather than an epitaxial overlayer. The Fe films were permanently magnetized in the plane of the sample by rare-earth magnets integrated into the sample holder that produce a magnetic field at the sample surface of $\approx$3 kG. Here MCD spectra were taken in the longitudinal geometry where the magnetization **M** is parallel to the reflecting surface and parallel to the plane of incidence defined by the incident light ray and the surface normal as shown in Fig. 1. The sample and detector assemblies can be rotated so that angles of incidence range from $\theta_i = 15°$ to 80° with respect to the sample normal.

MCD measurements at the $M_{2,3}$ edge of Fe were made *in situ* using a Si diode to measure consecutive reflected intensities for right- (RCP) and left-circularly polarized (LCP) light. Reflected intensities for LCP and RCP light differ near core absorption edges due to polarization-dependent transition probabilities.[22] It is convenient to quantify the MCD effect by normalizing the differences in intensities to the average reflected intensity:

$$\mathrm{MCD} = \frac{I_L - I_R}{\frac{1}{2}(I_L + I_R)}, \tag{1}$$

where I_L and I_R are the reflected intensities of LCP and RCP light. The monochromator was stepped incrementally through a photon energy range about the Fe absorption edge, and the QRP was positioned at angles $\pm\alpha$ with respect to the horizontal plane of the incoming linearly polarized light beam to supply LCP and RCP photons sequentially at each photon energy. The QRP was operated in a mode where the degree of circular polarization in the transmitted light was maximized. Over the photon energy range of interest, we kept $P_{\mathrm{circ}} \sim 0.98$. Since the time interval between the intensity measurement for each helicity is only a few seconds, normalization to the instantaneous stored beam current appeared to be unnecessary. When calculated in this manner, the MCD effect is independent of experimental conditions that change with time such as the absolute photon flux.

RESULTS AND DISCUSSION

In previous work, MCD spectra taken in the longitudinal geometry from macroscopically thick films at varying angles of incidence have been used to extract the frequency-dependent, complex dielectric tensor elements for Fe.[18] Once determined, the dielectric tensor, which governs the response of the material to incident electromagnetic radiation, can then be used to predict spectral line shapes and amplitudes for different experimental geometries.[23] In addition, as we present here, the dielectric tensor can be incorporated into a thin-film interference model to predict thickness-dependent alterations of in the MCD spectra of thin films. These analyses rely on a macroscopic approach based on the Maxwell-Fresnel formalism, which relates the dielectric properties to measurable quantities such as the absorbed or reflected light intensity. Relative to a microscopic model calculation, our approach does not directly allow easy access to material quantities such as the magnetic moment and its spin $\langle S_z \rangle$ and orbital $\langle L_z \rangle$ components. Despite this, the macroscopic model offers valuable insight into the angular- and thickness-dependent nature of MCD spectra which are not possible with the more elaborate microscopic theories.

Briefly, the macroscopic algorithm involves first calculating the reflection amplitudes for a vacuum-film interface for LCP and RCP light. Left- and right-circularly polarized light can be decomposed into s- and p-polarized components, al-

lowing the use of the familiar Fresnel reflection coefficients in calculating the reflection amplitudes. The *s* and *p* components are generated from the incident circularly polarized light using the change in bias

$$\begin{bmatrix} E_{\perp} \\ E_{\parallel} \end{bmatrix} = \begin{bmatrix} 1 \\ \pm i \end{bmatrix} E_0 , \tag{2}$$

where E_0 is the amplitude of the circularly polarized light. The reflection amplitudes perpendicular and parallel to the plane of incidence are then found from

$$\begin{bmatrix} R_{\perp} \\ R_{\parallel} \end{bmatrix} = \begin{bmatrix} r_{11} & r_{12} \\ r_{21} & r_{22} \end{bmatrix} \begin{bmatrix} E_{\perp} \\ E_{\parallel} \end{bmatrix}, \tag{3}$$

where the Fresnel reflection coefficients $r_{ij}=F_{ij}(\theta_i, n^*)$ depend on the angle of incidence θ_i and the complex index of refraction $n^*=n-ik$. Here the extinction coefficient k and index of refraction n are known from previous work[24] and are not treated as free parameters in the data reduction.

In this scheme, the reflected intensities for LCP and RCP light in terms of the Fresnel coefficients are

$$I_{L,R}=|r_{11}\pm ir_{12}|^2+|r_{21}\pm ir_{22}|^2. \tag{4}$$

For the longitudinal case $r_{21}=-r_{21}$ and, assuming $P_{\mathrm{circ}}=1$, the reflection coefficients can be written as

$$r_{11}=\frac{\cos\theta_i-n^*\cos\theta_t}{\cos\theta_i+n^*\cos\theta_t}, \tag{5}$$

$$r_{22}=\frac{n^*\cos\theta_i-\cos\theta_t}{n^*\cos\theta_i+\cos\theta_t}, \tag{6}$$

$$r_{12}=-r_{21}=\frac{\cos\theta_i\sin\theta_t}{\cos\theta_t(\cos\theta_i+n^*\cos\theta_t)(n^*\cos\theta_i+\cos\theta_t)}\,\frac{\varepsilon_{xy}}{\varepsilon_{xx}}, \tag{7}$$

where the angle of refraction θ_t is given by Snell's law $n^*=\sin\theta_i/\sin\theta_t$. Here the ε_{ij} are the frequency-dependent complex elements of the dielectric tensor that governs the propagation of electromagnetic radiation in the medium. For a ferromagnetic material magnetized in the *z* direction, the dielectric tensor can be written[1]

$$\overleftrightarrow{\varepsilon}=\begin{bmatrix} \varepsilon_{xx} & \varepsilon_{xy} & 0 \\ -\varepsilon_{xy} & \varepsilon_{xx} & 0 \\ 0 & 0 & \varepsilon_{zz} \end{bmatrix}. \tag{8}$$

The diagonal elements ε_{xx} and ε_{zz} account for the normal isotropic response of the medium to electromagnetic radiation. The nonzero off-diagonal elements, introduced by the magnetic nature of the medium, can be written as $\varepsilon_{xy}=\varepsilon_{xy}^1+i\varepsilon_{xy}^2$, and their frequency dependence can be found by a least-squares fit of the complete angular-dependent experimental MCD data set to the reflection equations, Eqs. (4)–(7). Previous experimental work has accomplished this for macroscopically thick Fe films.[18] No account of the thin-film interference effects, as outlined below, need be taken in the thick-film case because absorption within the film prevents interference between differently propagating rays of light.

The experimentally determined frequency-dependent dielectric tensor can then be used to predict the dependence of the longitudinal MCD effect as a function of film thickness in a classic thin-film interference model. Figure 1 shows a schematic of the interference process that occurs between light reflected from the vacuum-film interface and light reflected from the film-substrate interface (and additional multiple reflections). The substrate, which is nonmagnetic, enters the calculation simply via its complex index of refraction which determines the fraction of incident flux reflected at the film-substrate interface. The presence of the substrate does not influence the essential results reported here—similar effects would be noted for a freestanding film with vacuum interfaces at both surfaces. Note that due to the presence of the additional film-substrate interface, four different electromagnetic fields appear in the film—two propagating down into the substrate and two upward through the film. These four fields must satisfy the boundary conditions (the continuous variation of the tangential components of the electric and magnetic fields) at both interfaces. To consider the total power involved in the process, one must take into account the incident, reflected, and transmitted fields. This leads to a set of eight complex equations that need to be solved simultaneously in order to compute the thickness-dependent reflectance *R* or the absorbance *A* for both *s*- and *p*-polarization directions. Details of these calculations can be found in Ref. 25.

For a nonmagnetic film, the path differences between the multiple rays reflected towards the detector cause interference that would result in oscillatory intensity measurements as a function of film thickness. Most importantly, these variations in reflected light intensity would be identical for LCP and RCP light, and no change in MCD signal strength would be observed because the changes in LCP and RCP intensity would be in phase and of the same amplitude. However, the ferromagnetic Fe film is birefringent and therefore induces path differences for the multiple reflected rays that are different for light of opposite helicities. As a result, the classic thin-film interference phase difference is both thickness and polarization dependent. Therefore, because of the relationship expressed in Eq. (1), a modulation of the MCD effect is expected as the ferromagnetic film is grown. Of course, the MCD spectra also depend on the angle of incidence, which determines the path difference between the rays. It is essential to note, however, that for a fixed angle of incidence the model predicts changes in the MCD spectra without requiring a change in the magnetic properties of the film.

Interestingly, because of the frequency dependence of the dielectric tensor $\varepsilon(\omega)$, the characteristics of the modulated MCD effect depend on the photon energy. Figure 2 shows three graphs of the MCD effect which were calculated for slightly different photon energies as a function of film thickness. The calculations were performed for Fe films supported by a Cu substrate with an angle of incidence $\theta_i=45°$. The film thickness is reported in normalized units $t=d/\lambda$, where λ is the wavelength of the excitation energy. The curves for 52-, 53-, and 54-eV photons show damped, periodic oscillations as the film thickness increases. The oscillations are a direct result of the different response of the Fe film to the LCP and RCP light. As Fig. 2 shows, the magnitude of these

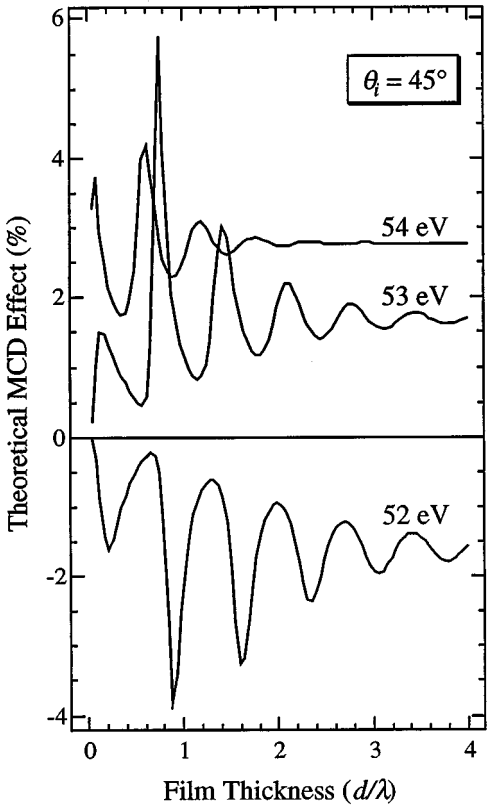

FIG. 2. Theoretical MCD effect as a function of film thickness in normalized units for $h\nu = 52$, 53, and 54 eV. These curves are calculated using the macroscopic Maxwell-Fresnel model and experimentally determined complex dielectric tensor elements of Fe around the $M_{2,3}$ region. The model incorporates interference effects between light reflected from the vacuum-film and film-substrate interfaces (Fig. 1). The phase differences between these rays are different for LCP and RCP light, giving rise to oscillations in the MCD effect which is calculated as $\mathrm{MCD} = 2*(I_L - I_R)/(I_L + I_R)$.

oscillations can easily exceed a 100% deviation from the steady-state MCD effect achieved for very thick films (i.e., where the reflection intensity from the buried film-substrate interface becomes insignificant due to absorption in the film). Significantly, for these curves the oscillations are out of phase and have different attenuation rates with increasing film thickness. Their characteristics result in a complex dependence of the MCD spectral line shape for a given film thickness and angle of incidence. It should be noted that the scale in Fig. 2 is a direct result of the calculations described above. There is no scaling to bulk films involved; the percent MCD effects reported are absolute.

By calculating a complete family of curves such as those in Fig. 2 over a photon energy range of 45–63 eV, we can generate theoretical MCD spectra at the $M_{2,3}$ edge for different film thicknesses. This is accomplished by inverting the specific-photon-energy versus film thickness matrix into a specific-thickness versus photon energy matrix. This procedure is equivalent to drawing a vertical line in Fig. 2 for the desired film thickness and recording the MCD effect at each photon energy, thereby generating a standard MCD spectrum. Several such theoretical MCD spectra for $\theta_i = 45°$ are shown in Fig. 3 where the film thickness is again reported as the normalized thickness $t = d/\lambda$.

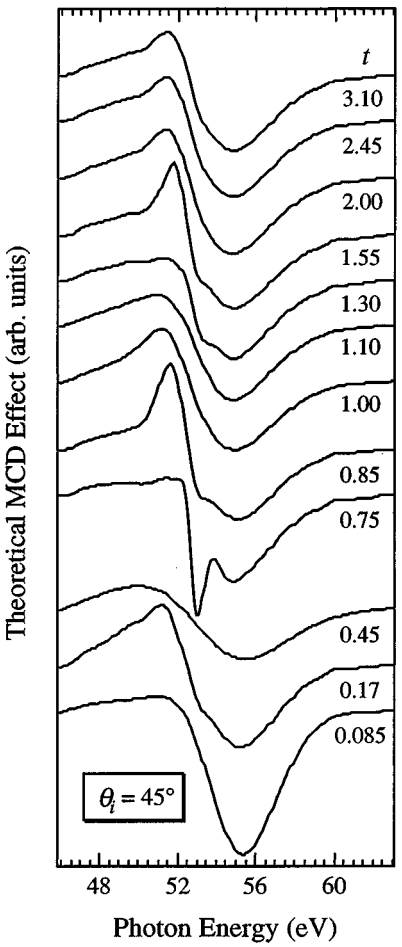

FIG. 3. Theoretical MCD spectra at different normalized thicknesses for Fe films supported by a Cu substrate. Families of thickness-dependent MCD effect curves such as those in Fig. 2 are ''inverted'' to yield energy-dependent line shapes at particular thicknesses. Significant variations in spectral line shape occur as the film thickness increases.

Figure 3 demonstrates that even though the angle of incidence and the magneto-optical characteristics are fixed, substantial variations in line shape occur as the film thickness increases. Some of the changes occur over very short thickness ranges; for example, a sharp leading edge feature appears and subsides near $t = 0.85$ and again at $t = 1.55$. A broad cycle of changes is observed to repeat as the path difference between rays reaches integral wavelengths—approximately every 225 Å for absorption at the $M_{2,3}$ edge of Fe. The primary periodic property is the change from a mostly negative line shape (at $t \approx 0.085$ and again at $t \approx 1.30$) to a more typical classic MCD line shape with both positive and negative peaks (at $t \approx 1.00$ and again at $t \approx 2.00$). As expected, the line shape reaches a steady state for thicker films ($t = 3.10$) where the differences in the LCP and RCP interference effects are negligible. Line shape changes such as the ones calculated and shown in Fig. 3 are not expected from a simple MCD theory, and if they are experimentally verified, it would necessitate a significant modification in the standard implementation of MCD experiments aimed towards investigations of the thickness-dependent magnetic properties of ultra thin films.

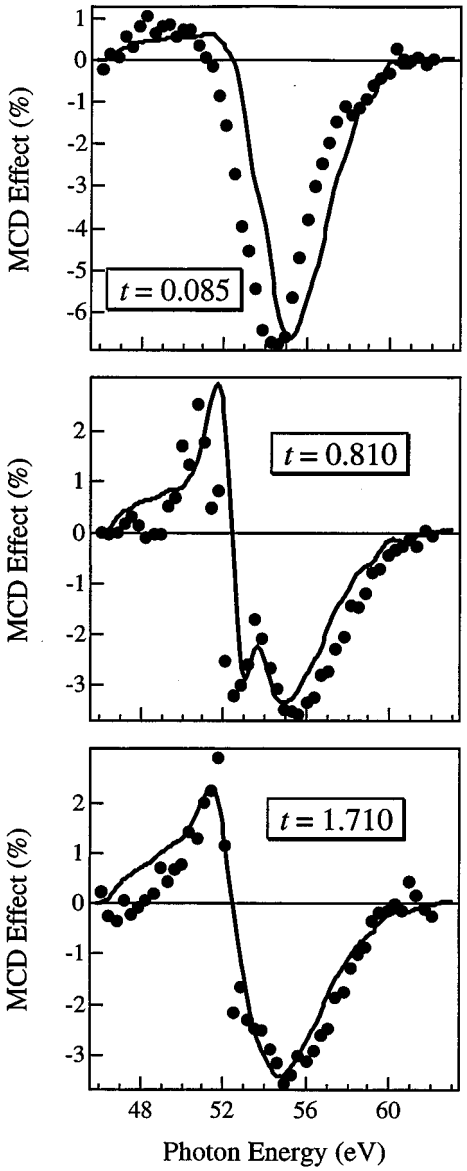

FIG. 4. Comparison between measured and predicted MCD spectra for Fe at normalized thicknesses of $t=0.085$, 0.810, and 1.710. The MCD spectra were measured using the reflected light mode at an angle of incidence of 45°. General spectral features, which show significant thickness dependence, are reproduced in the experimental curves, confirming the utility of the macroscopic model calculation.

The general features and trends present in the theoretical curves of Fig. 3 are reproduced in experimental MCD spectra as shown in Fig. 4, which displays several theoretical MCD spectra along with their experimentally measured counterparts. In general, the agreement between predicted and measured MCD curves is good. Distinctive features such as the sharp maximum and doubled negative structure for $t=0.810$ are reasonably reproduced in the experiment. In addition to line shape similarities, agreement between the theoretical and measured MCD effect magnitudes is also close. A factor of 0.85 was necessary to normalize the curves. This value is constant as a function of film thickness, indicating that a consistent source of error is present. Currently, we believe that this is not an artifact of the calculations, but

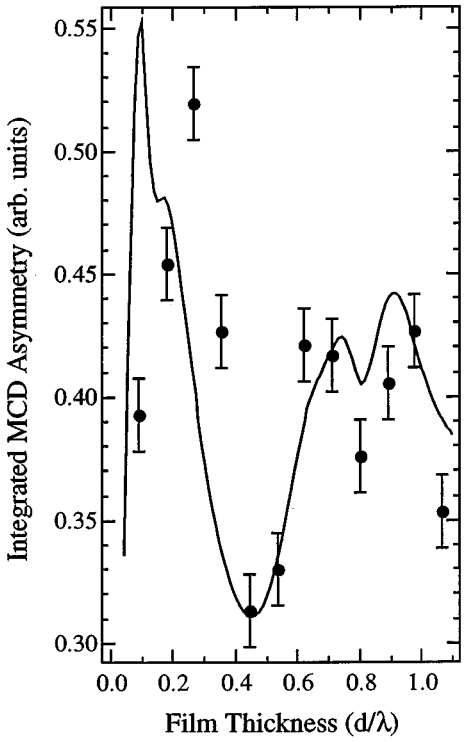

FIG. 5. Theoretical and measured integrated MCD effects for thin Fe films in the longitudinal geometry at 45° incidence. Variations in the thickness-dependent MCD effect are accounted for by the macroscopic theory described in the text, which demonstrates that they arise from thin-film interference effects rather than from varying magnetic moments.

rather related to the different surface properties of the Fe films of this investigation and the bulklike films grown earlier for the analysis of the dielectric tensor properties.[18]

Again, the emphasis here is on the variability in the predicted and measured MCD spectra. A striking progression of changes in line shape occurs as the film thickness increases which are not predicted by the basic MCD theory. Because they can be accounted for by the macroscopic theory that we have applied, we conclude that the variations in line shape are due to the geometric factors considered in the interference analysis—namely, film thickness and angle of incidence—rather than changes in the magnetic properties of the films.

As mentioned previously, the MCD spectrum from a ferromagnetic material can be related to the local magnetic environment through appropriate sum rules. Two of the characteristics of MCD spectra that can be considered in such an analysis are the peak-to-peak MCD difference of the spectrum and the integrated absolute area under the MCD energy spectrum. By virtue of the modulations in the MCD effect at a particular photon energy noted in Fig. 2, these important measures will also show variations with film thickness.

Figure 5 shows a comparison between the theoretical and measured integrated absolute MCD effect as a function of film thickness up to a thickness of $t\approx1.20$. Again, we find that basic features predicted by our model calculations are verified by the experiments. Starting from very thin films, the integrated MCD effect increases and then comes to a minimum around a thickness equivalent to about $\lambda/2$ of the exci-

tation wavelength. Less pronounced features such as the weaker minimum at $t \sim 0.8$ are also mirrored in the experiments. The slightly more pronounced discrepancies seen for the extreme thin films might be related to the formation of a thin contamination layer at the surface whose influence is gradually reduced with increasing thickness of the Fe film. Another source for the observed discrepancies for extremely thin films is related to the shortcomings of the macroscopic theory which ignores any surface effects and models the film with bulklike dielectric properties. Despite these model-limited shortcomings for films of a few monolayers thickness, the good overall agreement over a wide thickness range with various features of the experimental data indicates the general applicability of the simple macroscopic model to demonstrate the importance of interference effects in thin-film MCD experiments.

CONCLUSIONS

MCD experiments at the $M_{2,3}$ transition of thin Fe films show characteristic thickness-dependent variations of the MCD effect. The observed phenomena can be modeled using a simple macroscopic approach based upon the Maxwell-Fresnel formalism. The measurements show that interference effects can be very pronounced and if not properly accounted for could compromise any quantitative attempt to associate variations in the MCD effect solely to changes in the magnetic structure and moment distribution in ultrathin films. The problem of mixed contributions from simple thickness-dependent interference effects with real changes in the magnetic film properties is most severe for experiments involving the $L_{2,3}$ transitions. For the ferromagnetic $3d$ metals, these edges are at a wavelength region ranging from $\lambda \sim 17$ to 14 Å, which overlaps the strongest interference effects with the thickness-dependent changes in the magnetic material properties of films of several monolayer thickness. Because the model calculations consider the total power distributed into the reflected and absorbed light beam, the results presented here are not limited to reflection MCD, but are also applicable to total-electron-yield-absorption-type MCD experiments.

ACKNOWLEDGMENTS

This work is based upon research conducted at the Synchrotron Radiation Center, University of Wisconsin-Madison, which is supported by the NSF under Award No. DMR-95-31009. This work was supported in part by a Cottrell College Science Award of Research Corporation and the UW-Oshkosh Faculty Development Program.

[1] J. L. Erskine and E. A. Stern, Phys. Rev. B **12**, 5016 (1975).
[2] G. Schütz, W. Wagner, W. Wilhelm, P. Kienle, R. Zeller, R. Frahm, and G. Materlik, Phys. Rev. Lett. **58**, 737 (1987).
[3] S. P. Collins, M. J. Cooper, A. Brahmia, D. Laundy, and T. Pitkanen, J. Phys., Condens. Matter. **1**, 323 (1989).
[4] L. M. Falicov, D. T. Pierce, S. D. Baker, R. Gronsky, K. B. Hathaway, H. J. Hopster, D. N. Lambeth, S. S. P. Parkin, G. Prinz, M. Salamon, I. K. Schuller, and R. H. Victora, J. Mater. Res. **5**, 1299 (1990).
[5] B. T. Thole, G. van der Laan, and G. A. Sawatzky, Phys. Rev. Lett. **55**, 2086 (1985).
[6] B. T. Thole, P. Carra, F. Sette, and G. van der Laan, Phys. Rev. Lett. **68**, 1943 (1992).
[7] J. B. Goedkoop, B. T. Thole, G. van der Laan, G. A. Sawatzky, F. M. F. de Groot, and J. C. Fuggle, Phys. Rev. B **37**, 2086 (1988).
[8] P. Carra, B. T. Thole, M. Altarelli, and X. Wang, Phys. Rev. Lett. **70**, 694 (1993).
[9] B. T. Thole and G. van der Laan, Phys. Rev. Lett. **70**, 2499 (1993).
[10] G. van der Laan and B. T. Thole, Phys. Rev. B **53**, 14 458 (1996).
[11] C. T. Chen, F. Sette, Y. Ma, and S. Modesti, Phys. Rev. B **42**, 7262 (1990); C. T. Chen, Y. U. Idzerda, H.-J. Lin, N. V. Smith, G. Meigs, E. Chaban, G. H. Ho, E. Pellegrin, and F. Sette, Phys. Rev. Lett. **75**, 152 (1995).
[12] R. Wu, D. Wang, and A. J. Freeman, Phys. Rev. Lett. **71**, 3581 (1993).
[13] W. L. O'Brien and B. P. Tonner, Phys. Rev. B **50**, 12 672 (1994).
[14] A. Ankudinov and J. J. Rehr, Phys. Rev. B **51**, 1282 (1995).
[15] H. Höchst, R. Patel, and F. Middleton, Nucl. Instrum. Methods Phys. Res. A **347**, 107 (1994).
[16] D. C. Mancini, M. Bissen, D. Rioux, R. Patel, G. Rogers, E. L. Brodsky, and H. Höchst, Rev. Sci. Instrum. **63**, 1269 (1992).
[17] H. Höchst, P. Bulicke, T. Nelson, and F. Middleton, Rev. Sci. Instrum. **66**, 1598 (1995).
[18] H. Höchst, D. Zhao, and D. L. Huber, Surf. Sci. **252-254**, 998 (1996).
[19] D. A. Steigerwald, I. Jacob, and W. F. Egelhoof, Surf. Sci. **202**, 472 (1988).
[20] R. Naik, C. Kota, J. S. Payson, and G. L. Dunifer, Phys. Rev. B **48**, 1008 (1993).
[21] A. Chaiken, R. P. Michel, and M. A. Wall, Phys. Rev. B **53**, 5518 (1996).
[22] J. Stöhr and Y. Wu, in *New Directions in Research with Third-Generation Soft X-Ray Synchrotron Radiation Sources*, edited by A. S. Schlachter and F. J. Wuilleumier (Kluwer Academic, Boston, 1994), Vol. 254, pp. 221–250, and references therein.
[23] H. Höchst, D. Rioux, D. Zhao, and D. L. Huber, J. Appl. Phys. **81**, 7584 (1997).
[24] J. J. Carroll, C. T. Ceyer, and A. J. Melmed, J. Opt. Soc. Am. **72**, 668 (1978).
[25] D. Zhao, Ph.D. thesis, Department of Physics, University of Wisconsin-Madison, 1996.